

Strategy Based on Multiple Objectives and Null Space for the Formation of Mobile Robots and Dynamic Obstacle Avoidance

Leica P. *; Chavez D. **; Rosales A. **; Roberti F. †*; Toibero J. †*; Carelli R. †*

†Consejo Nacional de Investigación Científicas y Técnica

*Universidad Nacional de San Juan, Instituto de Automática, San Juan, Argentina

e-mail: (pleica,froberti,mitoibero,rcarelli)@inaut.unsj.edu.ar

**Escuela Politécnica Nacional, Facultad de Ingeniería Electrónica y Electrónica, Quito, Ecuador

e-mail: (danilo.chavez, andres.rosales)@epn.edu.ec

Resumen: En este trabajo se presenta un nuevo algoritmo para el control de formación flexible de robots móviles basado en múltiples objetivos de control. La estrategia contempla el uso del espacio nulo de una matriz Jacobiana para el control de forma y postura. La estrategia de evasión de obstáculos está basada en la definición de energía potencial ficticia. Se establece como objetivo primario el control de forma y evasión de obstáculos, y como objetivo secundario el control de postura y seguimiento de trayectoria de la formación de los robots. Se analiza la estabilidad de los controladores implementados y se presentan los resultados obtenidos por simulación que muestran el correcto desempeño de los controladores.

Palabras clave: Formación de robots, evasión de obstáculos, función potencial, seguimiento de trayectoria, espacio nulo.

Abstract: In this paper, a new algorithm for controlling mobile robot flexible formation based on multiple control objectives is presented. The strategy includes the use of null space for shape and posture control. The obstacle avoidance strategy is based on the definition of fictitious potential energy. The primary objective established is to shape control and obstacle avoidance, whereas the secondary objective includes the posture control and trajectory tracking of the robot formation. Stability analysis of the proposed control system is proven. Simulation results show the performance of the proposed controllers.

Keywords: robot formation, obstacle avoidance, potential function, trajectory tracking, null space.

1. INTRODUCTION

One of the current challenges in robotics is the cooperative control of multiple robots with a common goal. The possibility of making several smaller capacity robots to perform tasks that would be impossible or inefficient individually, has motivated the scientific community to encourage the development of innovative control strategies. The use of multiple robots versus one offers several advantages, which could include reduced costs, greater robustness, improved performance and efficiency [15]. Instead of designing a single specialized powerful robot, a multi-robot system can be simpler and less costly [12]. This feature has allowed formation control to be successfully used in various applications: military [18], civil [17] and service robotics. There are three basic structures in the bibliography. The control of multi-robot systems: leader-follower strategy, methods based on behavior and virtual structures, each with their respective advantages and disadvantages. In the leader-follower structure, an agent is considered the leader and the remaining agents are considered followers of the designated leader [7] and [8]. In this structure, only the follower has information about the leader, so if it fails there is no possible

mechanism that would ensure the compliance of the control target. However, this structure is easy to understand and implement. In the structure based on behavior, group behavior is defined as a combination of individual behavior of its members [5]. The main problem with this approach, is the difficult mathematical formalization and therefore it is not easy to ensure the convergence of the formation to the desired setting. In virtual structures geometry maintains a rigid connection between the robots and the reference system, which can be a virtual point or a virtual agent. One advantage of this method is that the virtual leader would never fail, so training will be maintained during the execution of the task.

Formations are categorized as rigid or flexible [14]. Working with rigid formations is advantageously less complex in terms of representation and control. The main disadvantage is that it may suffer collisions and encounter mobility problems, especially in corners and narrow passages, where the formation is larger than the available space [6]. In [13] a control scheme based on virtual structure is called cluster space control. Position control (or trajectory tracking) is carried out considering the centroid of the geometrical structure (a triangle) corresponding to the formation of three robots. In [16] the problem inherent in centralized control systems is addressed. More specifically, a technique to

extrapolate intrinsic generalization capabilities not discussed in [13] is developed, allowing application of the control approach based on the centroid of the formation in formations with a number equal to or greater than three robots. It also analyzes the ability of the formation in obstacle avoidance, whereby it can modify its structure momentarily, allowing an elastic behavior. At present the implementation of tasks in which robots are used requires extensive data processing in real time, while meeting a variety of tasks (manipulation, exploration, obstacle avoidance, etc.). This means that one must achieve several control goals simultaneously, sometimes causing conflict between them and the assigned order of priority. In [1] a number of control schemes are discussed that decompose the control problem into several sub-problems that are eventually solved individually.

Among the options, the control based on null spaces is enunciated, where the primary and most important objective is considered a minimum norm solution obtained by the pseudo-inverse of the Jacobian associated with the problem whereas the secondary objectives are posed in the null space of the aforementioned Jacobian. The main advantage is that this control scheme guarantees the fulfillment of the primary or higher priority, while the lower-level objectives should be analyzed in each case, but are projected in a space (null space) where it does not conflict with the main objective [3]. This concept was introduced in [2] to control generic robotic systems and in [4] to control multi-robotic systems. By interacting in dynamic and non-structured environments, multi-robot systems need to preserve their integrity, thus necessitating tools for obstacle avoidance. In bibliography, several proposals were found to solve this problem. One of them is the use of potential fields, as proposed in [9] and [10]. In this approach the obstacles generate repulsive forces on the robot, while the target generates attractive forces. The sum of all forces produces a resulting force that determines the direction and speed of the movement. Reference [11] analyzes the main limitations, among which the most important is the existence of local minimums that trap the robot, thus making it unable to reach the target. Another major limitation is the complication of passing through small spaces between obstacles, since they can generate repulsive forces greater than the attractive forces of the target. This paper presents a control scheme for tracking the formation of mobile robots, based on the null space of Jacobian matrix and the implementation of fictitious potential fields for obstacle avoidance. It is considered as a zero potential region to the entire environment with no barriers and non-zero in those regions containing obstacles. Then two control objectives are posed: a primary objective is to maintain the shape in areas of zero potential (without obstacles), and a secondary objective is to control trajectory and posture training. When an obstacle is found, the fictitious potential is different from zero and the formation deforms to avoid collisions with obstacles (static and dynamic). For obstacle avoidance fictitious potential fields are used, by characteristically not presenting local minimums, thereby offering an advantage. In this work, the temporal variation of

the potential field (which is not covered in the literature of potential fields) is contemplated, allowing introduction of the dynamic of moving obstacles. A new approach in the analysis of potential fields is presented, using the derivatives of the field in the trajectories of the system. Consequently, this work aims to solve the problem of controlling a formation of mobile robots in unstructured environments, using null spaces for multiple control objectives, incorporating the dynamics of the obstacles in a single controller. The main contribution of the paper is to present a methodology considering multiple-control objectives using the null space of a Jacobian matrix associated with the definition of an artificial potential and its temporal variation linked to the primary target.

The paper is organized as follows: Section 2 presents statement of the problem, the structure of the robot, the potential function and the robots formation implemented. In Section 3 the system is modeled. Section 4 develops control laws and their stability. Section 5 presents the simulation results. Finally, Section 6 concludes.

2. PROBLEM STATEMENT

2.1 Control Problem

While considering that two control objectives exist: the first combines obstacle avoidance (*Task 1*) and control shape (*Task 2*), whereas the second control objective combines trajectory tracking and posture angle of the formation (*Task 3*). This paper focuses on solving the trajectory tracking of mobile robotic formation with obstacle avoidance, using the concept of multiple-control objectives within the null space of the system. It is proposed that the centroid of the robot formation moves through a desired trajectory in an environment with obstacles. Trajectory tracking is part of one of the control tasks, which will be detailed later. The obstacle avoidance here is based on a fictitious potential field $\phi_{t,x}$ which includes the positions of the robots in the formation and obstacles external to it. In the absence of obstacles $\phi_{t,x} = 0$ and robots of the formation can navigate fulfilling the control objectives for shape and posture. In the presence of obstacles $\phi_{t,x} \neq 0$, the formation deforms to avoid hitting obstacles. For potential field generation only fictitious position obstacles and robots are required. However, if the variation of the potential field time $\partial\phi_{t,x}/\partial t$ is considered, it includes the dynamic behavior of the obstacles.

2.2 Potential Function

One of the control objectives is obstacle avoidance, requiring definition of a fictitious potential field that can describe a region of repulsion over the static or mobile obstacles. Potential function $\phi_{t,x}$ must describe the size of different obstacles within the environment, for which the following function has been adopted:

$$\phi_{t,x} = \begin{cases} r_v e^{-\frac{(x(t)-x_o(t))^2}{l_v^2} - \frac{(y(t)-y_o(t))^2}{p_v^2}} + \varepsilon (x(t) + y(t)) - r_o & ; C_1 \\ 0 & ; C_2 \end{cases} \quad (1)$$

where $\varepsilon \ll r_o$; $0 < r_o \ll r_v$; $C_1 = l_v < l_o$, $p_v < p_o$; $C_2 = l_v > l_o$, $p_v > p_o$; r_v, l_v and p_v are parameters that describe the object size; $x_o(t)$ and $y_o(t)$ are the coordinates of the obstacle in the world, $x(t)$ and $y(t)$ are the coordinates in the world. Figure 1 shows the shape of the potential function for an obstacle.

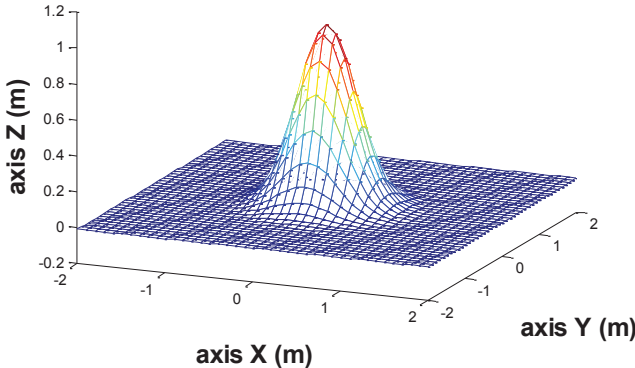


Figure 1. Shape of the potential function $\phi_{t,x}$ ($l_o = p_o = 0.35$; $r_v = 1$)

2.3 Mobile Robot

This paper uses unicycle-like mobile robots (see Figure 2) whose kinematic model is given as follows by:

$$\begin{bmatrix} \dot{x}_i \\ \dot{y}_i \\ \dot{\psi}_i \end{bmatrix} = \begin{bmatrix} \cos(\psi_i) & -a \sin(\psi_i) \\ \sin(\psi_i) & a \cos(\psi_i) \\ 0 & 1 \end{bmatrix} \begin{bmatrix} u_i \\ \omega_i \end{bmatrix} \quad (2)$$

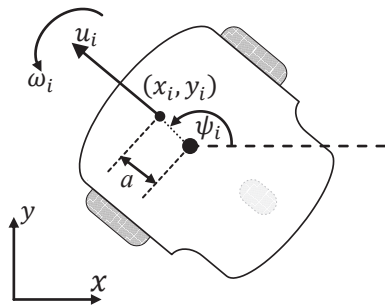


Figure 2. One-cycle type mobile robot

where a is the displacement of this point of interest (x_i, y_i) on the longitudinal axis of the i -th robot to the midpoint between the wheels; ψ_i is the orientation of the i -th robot; u_i and ω_i are the linear and angular velocities of the i -th robot respectively. For control purposes, the kinematics can be described in a compact form with (3) and (4) without the $\dot{\psi}_i$, because of the non-holonomic characteristic of the mobile robot, the only way to navigate the zero position error path is when the robot has the same orientation as the path or trajectory. Where $\dot{X}_i = [\dot{x}_i \quad \dot{y}_i]$ are the temporal variations of the i -th position robot; $U_i = [u_i \quad \omega_i]$ are the i -th speeds.

$$\begin{bmatrix} \dot{x}_i \\ \dot{y}_i \end{bmatrix} = \begin{bmatrix} \cos(\psi_i) & -a \sin(\psi_i) \\ \sin(\psi_i) & a \cos(\psi_i) \end{bmatrix} \begin{bmatrix} u_i \\ \omega_i \end{bmatrix} = J_{ri} \begin{bmatrix} u_i \\ \omega_i \end{bmatrix} \quad (3)$$

$$\dot{X}_i = J_{ri} U_i \quad (4)$$

2.4 Robot Formation

This paper proposes to work with the formation disposed according to Figure 3, where d_1 is the distance between robots R_1 and R_3 ; d_2 is the distance between robot R_1 and R_2 , d_3 is the distance between the robot and R_2 and R_3 , β is the angle opposite to the d_3 segment; x_c and y_c are the positions of the centroid of the formation in reference to the world; θ is the formation posture angle. Thus the shape variables are defined by $q_f = [d_1 \quad d_2 \quad \beta]^T$ and the posture variables by $q_p = [x_c \quad y_c \quad \theta]^T$, where $q = [q_f \quad q_p]$, being:

$$q_f = \begin{bmatrix} d_1 \\ d_2 \\ \beta_1 \end{bmatrix} = \begin{bmatrix} \sqrt{(x_1 - x_3)^2 - (y_1 - y_3)^2} \\ \sqrt{(x_1 - x_2)^2 - (y_1 - y_2)^2} \\ \arccos \left(\frac{d_1^2 + d_2^2 - d_3^2}{2 d_1 d_2} \right) \end{bmatrix} \quad (5)$$

$$q_p = \begin{bmatrix} x_c \\ y_c \\ \theta \end{bmatrix} = \begin{bmatrix} \frac{x_1 + x_2 + x_3}{3} \\ \frac{y_1 + y_2 + y_3}{3} \\ \arctan \left(\frac{\frac{2}{3}x_1 - \frac{1}{3}(x_2 + x_3)}{\frac{2}{3}y_1 - \frac{1}{3}(y_2 + y_3)} \right) \end{bmatrix} \quad (6)$$

where $R_1 = (x_1, y_1)$; $R_2 = (x_2, y_2)$ and $R_3 = (x_3, y_3)$.

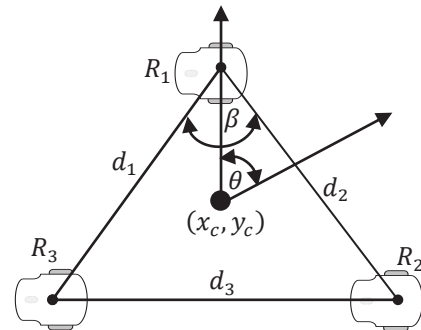


Figure 3. Robot formation diagram

This formation was selected because it can express the shape variables and posture variables separately. This allows to obtain multiple control objectives using the null space of the system. It should be clarified that, the formation can have more than three robots, but it is should consider changes in q_f and q_p .

3. SYSTEM MODELING

3.1 Kinematic Modeling of the System

The structure of the control system is shown in Figure 4, where the generation of multiple tasks is performed by the

concept of multiple control targets using the null space of the system. J_1 is the Jacobian that relates the tasks velocities with velocities of each robot.

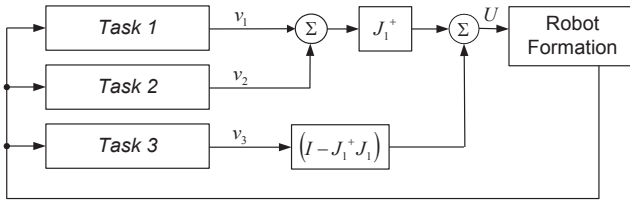


Figure 4. Control diagram structure

Task 1 is to avoid obstacle collision, *Task 2* is to keep the shape q_f of robot formation and *Task 3* is to follow a desired trajectory while maintaining the posture angle of the formation. The variables v_1 , v_2 and v_3 represent the velocities generated by each task to meet the control objectives. Vector $U = [u_1 \omega_1 u_2 \omega_2 \dots u_n \omega_n]$ contains linear and angular velocities of the robots included in the formation and can be defined as:

$$U = J_1^+(v_1 + v_2) + (I - J_1^+J_1)v_3 \quad (7)$$

Equation 7 describes the overall control system structure in general, the same that will be placed depending on the variables such as shape q_f and posture q_p , which is detailed as follows.

Firstly, *Task 2* is analyzed and is defined as a function of posture variables q_f :

$$\dot{q}_f = J_f \dot{X} \quad (8)$$

where:

$$J_f = \begin{bmatrix} \frac{\partial d_1}{\partial x_1} & \frac{\partial d_1}{\partial y_1} & \frac{\partial d_1}{\partial x_2} & \frac{\partial d_1}{\partial y_2} & \dots & \frac{\partial d_1}{\partial x_n} & \frac{\partial d_1}{\partial y_n} \\ \frac{\partial d_2}{\partial x_1} & \frac{\partial d_2}{\partial y_1} & \frac{\partial d_2}{\partial x_2} & \frac{\partial d_2}{\partial y_2} & \dots & \frac{\partial d_2}{\partial x_n} & \frac{\partial d_2}{\partial y_n} \\ \vdots & \vdots & \vdots & \vdots & \ddots & \vdots & \vdots \\ \frac{\partial \beta}{\partial x_1} & \frac{\partial \beta}{\partial y_1} & \frac{\partial \beta}{\partial x_2} & \frac{\partial \beta}{\partial y_2} & \dots & \frac{\partial \beta}{\partial x_n} & \frac{\partial \beta}{\partial y_n} \end{bmatrix} \quad (9)$$

From linear algebra the minimum solution norm is defined by the right pseudo-inverse as $J_f^+ = J_f^T (J_f J_f^T)^{-1}$, thus the solution in the row space of J_f is defined by the system inverse kinematics as:

$$\dot{X} = J_f^+ \dot{q}_f \quad (10)$$

where $\dot{X} = [\dot{x}_1 \dot{y}_1 \dot{x}_2 \dot{y}_2 \dots \dot{x}_n \dot{y}_n]$. Replacing (10) according to structure (4) for n robots reveals the relationship between the shape variables and the velocities of the robots, defined by:

$$U = J_r^{-1} J_f^+ \dot{q}_f \quad (11)$$

Now, to enter the *Task 3* in (11) it is projected position variables in the null space of J_f . This will allow the formation to retain its shape, and also to retain its posture along a desired trajectory. Thus (11) can be rewritten as:

$$U = J_r^{-1} (J_f^+ \dot{q}_f + (I - J_f^+ J_f) \dot{X}_p) \quad (12)$$

being:

$$\dot{X}_p = J_p^+ \dot{q}_p \quad (13)$$

where $J_p^+ = J_p^T (J_p J_p^T)^{-1}$; \dot{X}_p are temporal variations of positions for the posture, and J_p is the Jacobian defined by:

$$J_p = \begin{bmatrix} \frac{\partial x_c}{\partial x_1} & \frac{\partial x_c}{\partial y_1} & \frac{\partial x_c}{\partial x_2} & \frac{\partial x_c}{\partial y_2} & \dots & \frac{\partial x_c}{\partial x_n} & \frac{\partial x_c}{\partial y_n} \\ \frac{\partial y_c}{\partial x_1} & \frac{\partial y_c}{\partial y_1} & \frac{\partial y_c}{\partial x_2} & \frac{\partial y_c}{\partial y_2} & \dots & \frac{\partial y_c}{\partial x_n} & \frac{\partial y_c}{\partial y_n} \\ \frac{\partial \theta}{\partial x_1} & \frac{\partial \theta}{\partial y_1} & \frac{\partial \theta}{\partial x_2} & \frac{\partial \theta}{\partial y_2} & \dots & \frac{\partial \theta}{\partial x_n} & \frac{\partial \theta}{\partial y_n} \\ \frac{\partial x_c}{\partial y_1} & \frac{\partial x_c}{\partial y_2} & \frac{\partial x_c}{\partial y_3} & \frac{\partial x_c}{\partial y_4} & \dots & \frac{\partial x_c}{\partial y_n} & \frac{\partial x_c}{\partial y_n} \\ \frac{\partial y_c}{\partial x_1} & \frac{\partial y_c}{\partial x_2} & \frac{\partial y_c}{\partial x_3} & \frac{\partial y_c}{\partial x_4} & \dots & \frac{\partial y_c}{\partial x_n} & \frac{\partial y_c}{\partial x_n} \\ \frac{\partial \theta}{\partial x_1} & \frac{\partial \theta}{\partial x_2} & \frac{\partial \theta}{\partial x_3} & \frac{\partial \theta}{\partial x_4} & \dots & \frac{\partial \theta}{\partial x_n} & \frac{\partial \theta}{\partial x_n} \end{bmatrix} \quad (14)$$

The system design is completed including obstacle avoidance (*Task 1*) to which a term is added to the shape variables \dot{q}_{ob} , moreover allowing static and dynamic obstacle avoidance by robots. Thus (12) is rewritten as:

$$U = J_r^{-1} (J_f^+ (\dot{q}_f + \dot{q}_{ob}) + (I - J_f^+ J_f) \dot{X}_p) \quad (15)$$

In the following the \dot{q}_{ob} is obtained.

3.2 Obstacle Avoidance

The control problem is to design a controller so multiple mobile robots can maintain their shape while its centroid follows a desired trajectory in a dynamic environment (with fixed and moving obstacles) and suggests that only robots can move into positions where the fictitious potential field $\phi_{t,x}$ is less than or equal to zero. This requires finding a relationship that associates the fictitious potential field of each obstacle to the movement of each robot in the formation. This can be obtained by setting the variation of the potential field on the basis of temporal variations in the robot position. Deriving $\phi_{t,x}$ in the \dot{X}_{ob} trajectories obtains:

$$\frac{d\phi_{t,x}}{dt} = \nabla \phi_{t,x} \dot{X}_{ob} + \frac{\partial \phi_{t,x}}{\partial t} \quad (16)$$

where \dot{X}_{ob} are temporal variations of the position of each robot to avoid collisions; $\nabla \phi_{t,x}$ is the partial derivative of $\phi_{t,x}$ with respect to the positions of each robot in the formation; $\partial \phi_{t,x} / \partial t$ is the potential field variation in time, this component provides dynamic information of the movement of the obstacles within the environment. Hence forth, $\nabla \phi_{t,x} = J_\phi$ is the Jacobian that relates the temporal variations of the field with temporal variations of the positions of each robot of the formation, and is expressed as follows:

$$J_\phi = \left[\frac{\partial \phi_{t,x}}{\partial x_1}, \frac{\partial \phi_{t,x}}{\partial y_1}, \dots, \frac{\partial \phi_{t,x}}{\partial x_n}, \frac{\partial \phi_{t,x}}{\partial y_n} \right] \quad (17)$$

The kinematics of the system is defined by:

$$\dot{\phi}_{t,x} = J_\phi \dot{X}_{ob} + \frac{\partial \phi_{t,x}}{\partial t} \quad (18)$$

From linear algebra it is known that the minimum norm solution is defined by the right pseudo-inverse $J_\phi^+ =$

$J_\phi^T (J_\phi J_\phi^T)^{-1}$, then the solution in the row space of J_v is defined by the inverse kinematics of the system as:

$$\dot{X}_{ob} = J_\phi^+ \left(\dot{\phi}_{t,x} - \frac{\partial \phi_{t,x}}{\partial t} \right) \quad (19)$$

Now, from (14) $\dot{q}_{ob} = J_f \dot{X}_{OB}$ is obtained and replacing (19) gives:

$$\dot{q}_{ob} = J_f J_\phi^+ \left(\dot{\phi}_{t,x} - \frac{\partial \phi_{t,x}}{\partial t} \right) \quad (20)$$

4. CONTROLLERS

4.1 Proposed Controller

To meet the three tasks, the following controller is suggested.

$$U_c = J_r^{-1} (J_f^+ (\dot{q}_{fc} + \dot{q}_{obc}) + (I - J_f^+ J_f) \dot{X}_{pc}) \quad (21)$$

being:

$$\dot{q}_{fc} = \dot{q}_{fd} + K_f \tanh \tilde{q}_f \quad (22)$$

$$\dot{q}_{obc} = J_f J_\phi^+ \left(\dot{\phi}_d + K_\phi \tanh \tilde{\phi}_{t,x} - \frac{\partial \phi_{t,x}}{\partial t} \right) \quad (23)$$

where K_f and K_ϕ are positive definite diagonal matrixes. The variables \dot{q}_{fd} and $\dot{\phi}_d$ are the temporal variations of the shape and obstacle avoidance variables respectively. The shape errors are defined as $\tilde{q}_f = q_{fd} - q_f$, where q_{fd} is the desired value of the shape $q_{fd} = [d_{1d} \ d_{2d} \ \beta_d]^T$.

Fictitious potential error $\tilde{\phi}$ is generated by the presence of obstacles and is defined by $\tilde{\phi} = \phi_d - \phi$ where ϕ_d is the desired potential function, in this case $\phi_d = 0$ (obstacle free potential), which means that the robot can only move in the position $(x(t), y(t))$ that are obstacle-free. The position controller is defined by:

$$\dot{X}_{pc} = J_p^+ (\dot{q}_{pd} + K_p \tanh \tilde{q}_p) \quad (24)$$

where K_p is a diagonal matrix defined as positive, the error position is defined by $\tilde{q}_p = q_{pd} - q_p$; where $q_{pd} = [x_{cd} \ y_{cd} \ \theta_d]^T$; temporal variations desired are defined by $\dot{q}_{pd} = [\dot{x}_{dc} \ \dot{y}_{dc} \ \dot{\theta}_d]^T$, where \dot{x}_{dc} and \dot{y}_{dc} are trajectory reference speeds.

4.1 Stability Analysis

This section analyzes the stability of the proposed controller. To clarify this analysis, the following definition is presented:

Definition: For any n by n matrix A , the null space and the row space are orthogonal sub-spaces of \mathcal{R}^m . Similarly the left null space and the column space are orthogonal sub-spaces of \mathcal{R}^n .

This means that $J_2 J_f^+ = 0$ because $\mathcal{R}(J_2^+) \subseteq I - J_f^+ J_f = \mathcal{N}(J_f)$, J_2 being the projection matrix in the null space of J_f .

First, it is analyzed the secondary objective (*Task 3*) that does not affect the primary endpoint (*Task 1* and *Task 2*). To demonstrate this (4) in (8) for n robots:

$$\dot{q}_f = J_f \ J_r \ U \quad (25)$$

Assuming perfect velocity tracking $U_c \equiv U$, replacing (21) in (25):

$$\dot{q}_f = J_f (J_f^+ (\dot{q}_{fc} + \dot{q}_{obc}) + (I - J_f^+ J_f) \dot{X}_{pc}) \quad (26)$$

Since it is known that $J_f^+ = J_f^T (J_f J_f^T)^{-1}$ by replacing in (26) and developing results in:

$$\dot{q}_f = (\dot{q}_{fc} + \dot{q}_{obc}) \quad (27)$$

This implies that the secondary target does not affect the primary objective.

Now the stability of the shape errors is analyzed. Assuming that there are no obstacles $\dot{q}_{obc} = 0$, and assuming perfect velocity tracking, by replacement of (22) in (27) results in:

$$\dot{q}_f = \dot{q}_{fd} + K_f \tanh \tilde{q}_f \quad (28)$$

The shape errors are defined by:

$$\dot{\tilde{q}}_f + K_f \tanh \tilde{q}_f = 0 \quad (29)$$

where $\dot{\tilde{q}}_f = \dot{q}_{fd} - \dot{q}_f$; as K_f is a positive defined diagonal matrix $\tilde{q}_f \rightarrow 0$ asymptotically in the absence of obstacles.

Now the stability of the position errors is analyzed. From (4) for n robots $\dot{X}_p = J_r U$, assuming perfect velocity tracking ($U \equiv U_c$) thus:

$$\dot{X}_p = J_f^+ (\dot{q}_{fc} + \dot{q}_{obc}) + (I - J_f^+ J_f) \dot{X}_{pc} \quad (30)$$

Replacing (13) in (30):

$$J_p^+ \dot{q}_p = J_f^+ (\dot{q}_{fc} + \dot{q}_{obc}) + (I - J_f^+ J_f) \dot{X}_{pc} \quad (31)$$

Multiplying both members of equality by $J_2 = I - J_f^+ J_f$ and developing them results in (see Appendix A):

$$J_A (\dot{\tilde{q}}_p + K_p \tanh \tilde{q}_p) = 0 \quad (32)$$

where $J_A = J_2 J_p^+$, which moreover verifies that the null space $N(J_f) = \{\dot{X}/J_f \dot{X} = 0\}$ has a dimension $\dim N(J_f) = 3$, which is logical because three shape variables are used in the primary objective and three variables are left free for posture. Now as in the secondary objective (posture) the three remaining free variables are used, it is observed that the null space $N(J_A) = \{\dot{X}/J_A \dot{X} = 0\}$ has a $\dim N(J_A) = 0$, this means that there are no free variables, therefore further object of control cannot be increased. In addition, its algebraic meaning signifies that the J_A matrix is a full range and the posture error system is defined by:

$$\dot{\tilde{q}}_p + K_p \tanh \tilde{q}_p = 0 \quad (33)$$

where K_p is a positive defined diagonal matrix, then $\tilde{q}_p \rightarrow 0$.

5. SIMULATION RESULTS

Simulations were performed using the Matlab computer program. The simulated robots incorporate a kinematic model of a non-holonomic robot (Pioneer 2 [19]). Two experiments were conducted: 1) It is proposed that the centroid of the robot formation moves through a desired trajectory in an environment with three obstacles (two static obstacles and one dynamic obstacle, see Figure 5), maintaining the formation and avoiding obstacles as a primary objective; and 2) It is proposed that the centroid of the robot formation moves through a desired trajectory in an environment with three robots (one fixed and two mobiles). The objective of this second experiment is to demonstrate control strategy behavior when the formation interacts with other robots having the same collision-avoidance strategy. All robots (six robots) react to avoid collisions between them, thus reducing control errors with respect to first experiment.

5.1 Experiment 1

The initial conditions of the robots formation are: $R_1 = (-1.5, 1)$; $R_2 = (-1, 1)$; $R_3 = (-1, -1.5)$; $\psi_1 = \psi_2 = -30^\circ$ and $\psi_3 = 0$ the initial positions of the objects are: $X_{ob,1} = (2.5, 2)$; $X_{ob,2} = (2, 0)$ and $X_{ob,3} = (10, 2)$, the speed of the dynamic object is 0.4 (m/s). The reference positions are: $\theta_d = 0^\circ$ and $(x_{dc}, y_{dc}) = (x_{ref}, y_{ref})$, where x_{ref} , y_{ref} corresponds to the reference trajectory given by $y = A \sin(\omega x)$ with $A = 1$, $\omega = \pi/4$. Shape references are: $d_{d1} = d_{d2} = 1.2$ (m) and $\beta_d = 60^\circ$.

Figure 5 shows the evolution of one experiment. Figures 6 and 7 show the evolution of shape errors and verify that in the absence of obstacle control, errors tend to be zero. Int = 9 (s) to $t = 17$ (s) errors occur due to the presence of two static obstacles, and in $t = 34$ (s) to $t = 37$ (s) the errors are due to the presence of the dynamic obstacle.

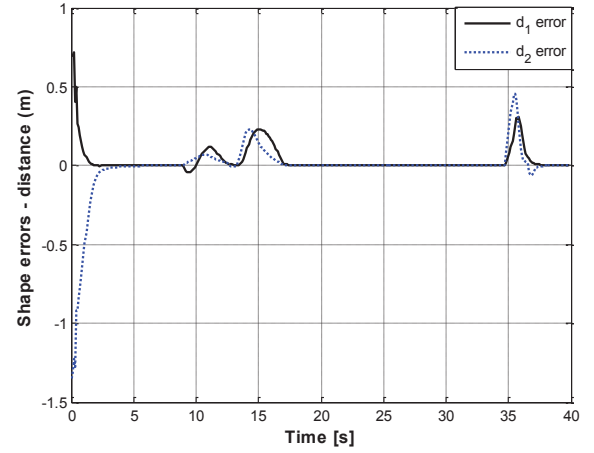


Figure 6. Evolution of the shape errors \tilde{d}_1 and \tilde{d}_2

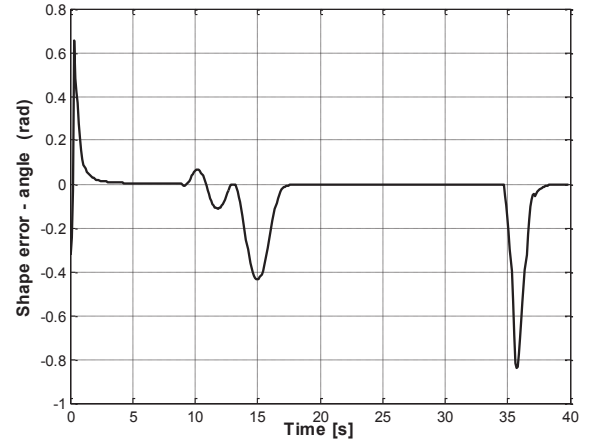


Figure 7. Evolution of the shape error $\tilde{\beta}$

Figure 8 shows the evolution of the posture error \tilde{x}_c and \tilde{y}_c corresponding to the trajectory reference errors. Figure 9 presents the evolution of $\tilde{\theta}$. It is observed that at $t = 9$ (s) to $t = 17$ (s) and from $t = 34$ (s) to $t = 37$ (s) errors appear in the presence of obstacles. In Figure 10 the evolution of the potential field is shown for the three formation robots, which verifies that the potential field isn't zero in presence of obstacles.

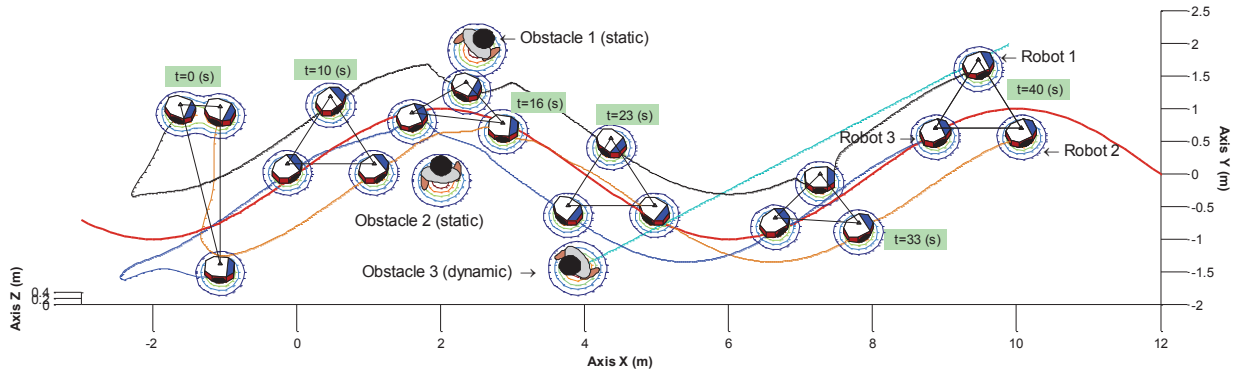


Figure 5. Positions and trajectories of obstacles and robots for experiment one

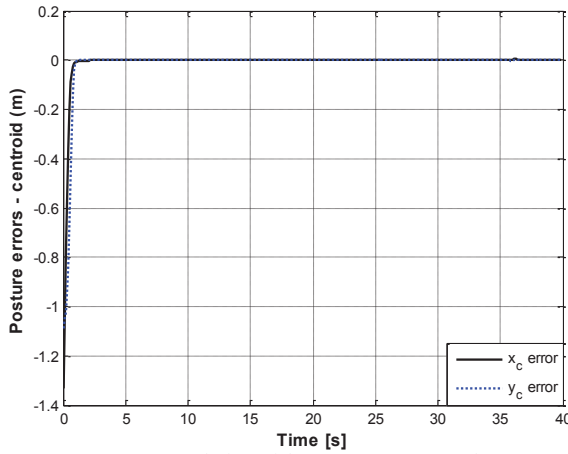


Figure 8. Evolution of the posture error \tilde{x}_c and \tilde{y}_c

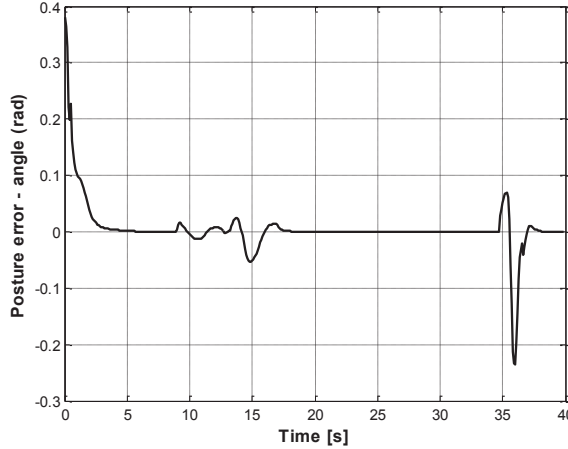


Figure 9. Evolution of the posture error $\tilde{\theta}$

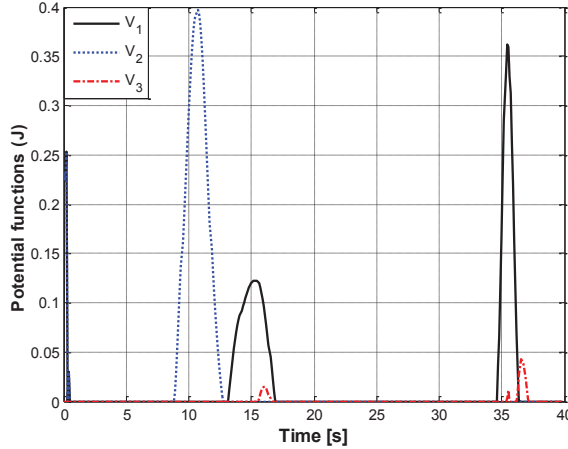


Figure 10. Evolution of each robots potentials functions

Figure 11 shows the evolution of time-parameterized trajectories of the robots and dynamic obstacle. The trajectories of the robots do not intersect with the obstacle, which implies that the formation of robots avoids collision with dynamic obstacle (obstacle 3). The collision avoidance for both static obstacles can be verified in Figure 5. The R_1 trajectory is of interest because it can collide with the dynamic obstacle. Figure 12 shows the difference in the

trajectories for the two cases: when $\partial\phi_{t,x}/\partial t = 0$ and when $\partial\phi_{t,x}/\partial t \neq 0$.

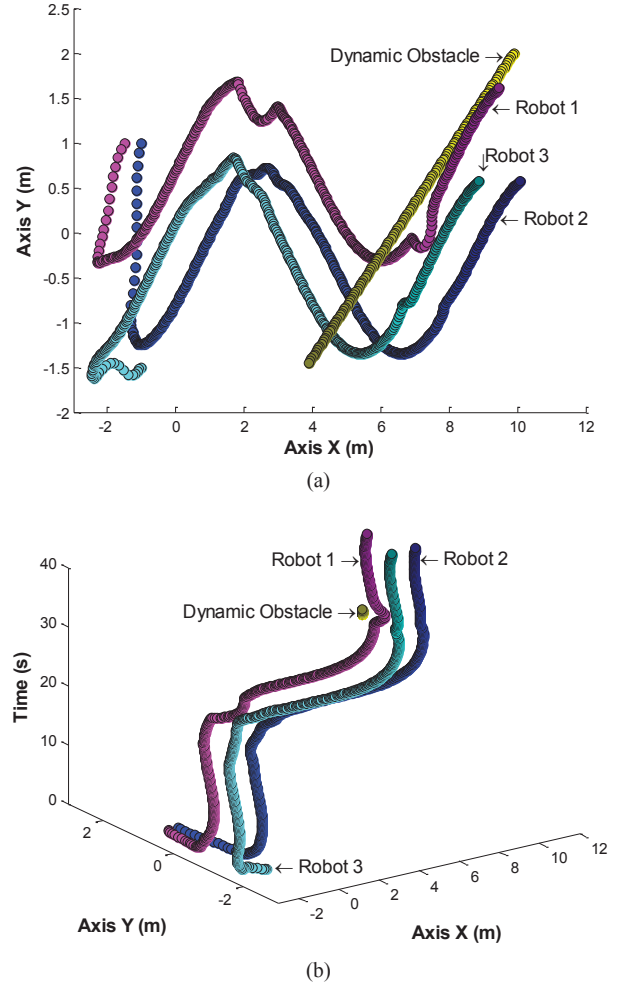
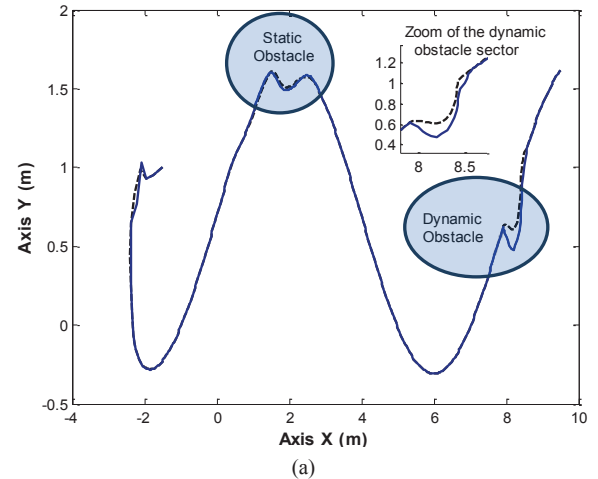


Figure 11. Time-Parameterized trajectories.a)Time-Parameterized trajectories [upper view]. b) Time-Parameterized trajectories [rotated view]



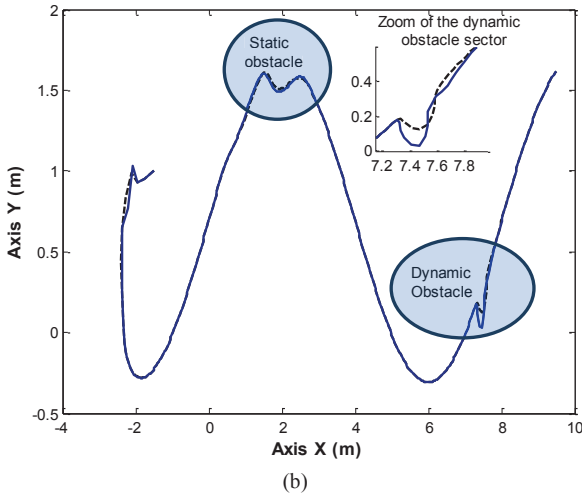


Figure 12. Trajectory-Evolution of the formation robots for $R_1.12.a)$ low speeds. $12.b)$ high velocities

Figure 12 shows the difference of the trajectory for R_1 when the variation of the potential field $\partial\phi_{t,x}/\partial t = 0$ (broken line) is not considered and when the variation of potential field $\partial\phi_{t,x}/\partial t \neq 0$ is considered (solid line). Figure 12(b) shows the trajectories of R_1 when the dynamic obstacle speed has increased three times [3x]. In that event, a major difference in both cases is observable. When $\partial\phi_{t,x}/\partial t = 0$ the robot R_1 touches the dynamic obstacle, however when $\partial\phi_{t,x}/\partial t \neq 0$ the robot swerves to avoid the dynamic obstacle, which would implicate the importance of the variation of the potential field for dynamic obstacles.

5.2 Experiment 2

The difference is that in the first experiment only the formation of robots (the three robots) react to avoid collision, while in the second experiment all robots (six robots) react to avoid collisions between them, thus reducing control errors with respect to first experiment (see Figures 14, 15, 16 and 17). The form, posture, and trajectory parameters are the same as in the previous experiment. The initial conditions of the three new robots are $R_4 = (10, 2)$; $R_5 = (2.5, 2)$; $R_6 = (9, -1.5)$; $\psi_{r4} = -145^\circ$, $\psi_{r5} = 0^\circ$ and $\psi_{r6} = 180^\circ$; the speeds of R_4 and R_6 are 0.6 (m/s) and 0.3 (m/s) respectively.

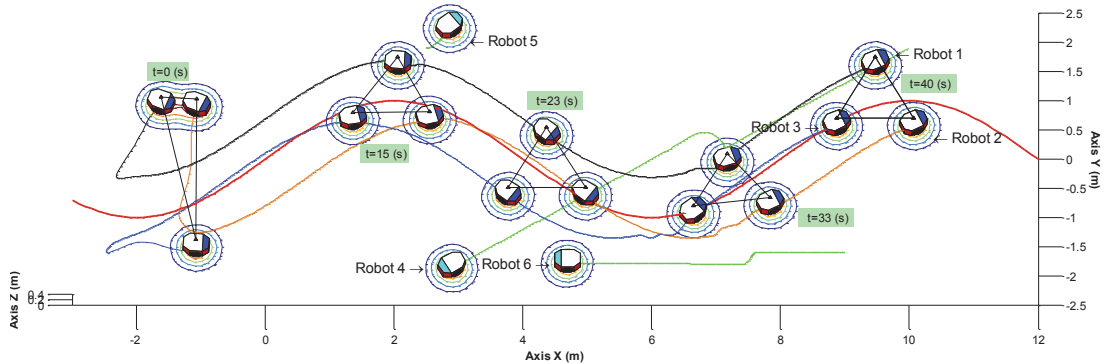


Figure 13. Positions and trajectories of obstacles and robots for experiment two

Figure 13 reveals the evolution of the second experiment. Figures 14, 15, 16 and 17 show the form and posture errors, observing their increase when avoiding the collision with robots encountered navigating within the same environment.

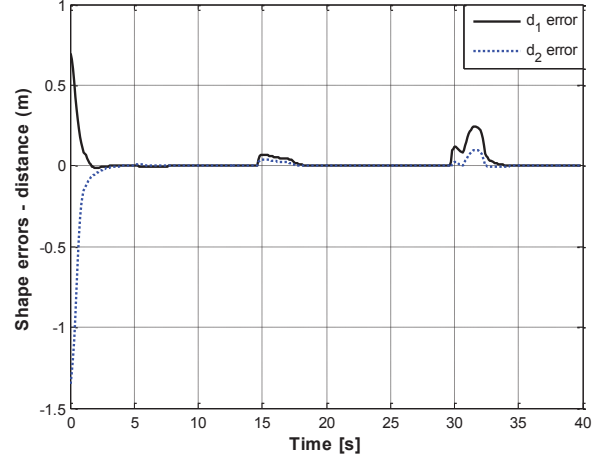


Figure 14. Evolution of shape error \tilde{d}_1 and \tilde{d}_2

The control errors presented in $t = 14$ (s) tot $= 17$ (s) are due to the possible collision with R_4 and in $t = 29$ (s) to $t = 33$ (s) are due to the possible collision with robots R_4 and R_6 .

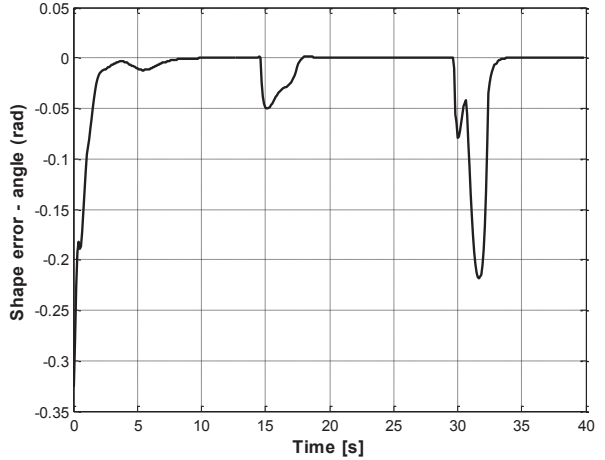


Figure 15. Evolution of shape error $\tilde{\beta}$

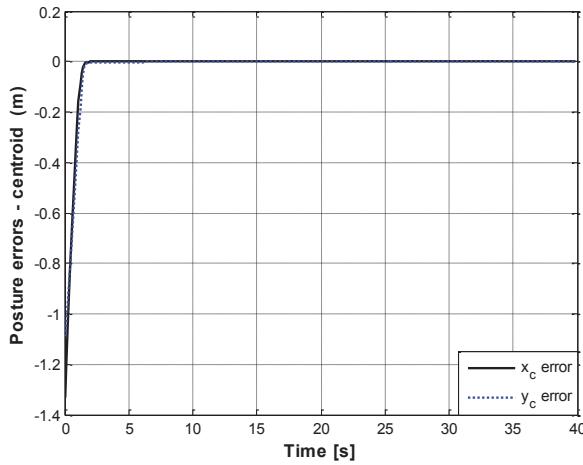


Figure 16. Evolution of posture errors \tilde{x}_c and \tilde{y}_c

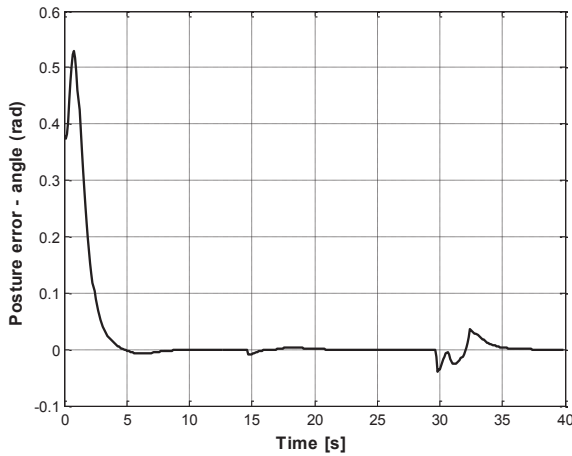
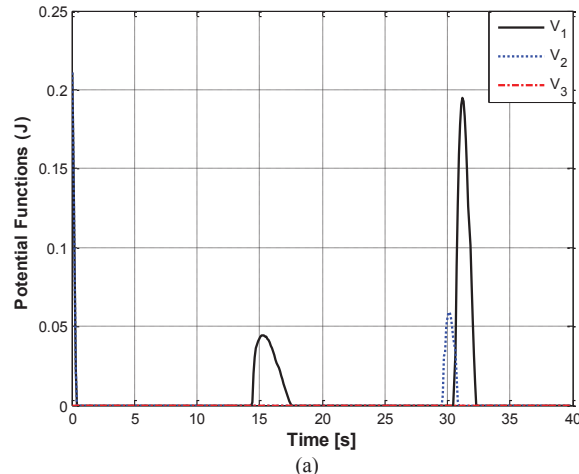
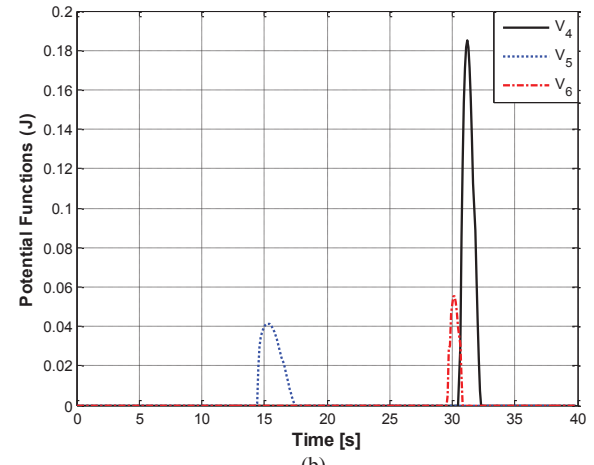


Figure 17. Evolution of posture errors $\tilde{\theta}$



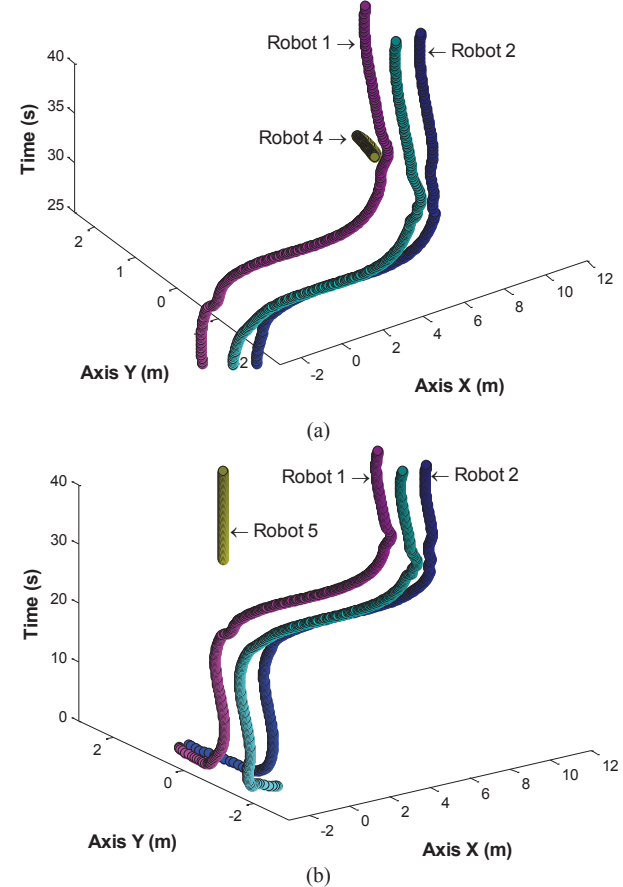
(a)



(b)

Figure 18. Evolution of the potentials functions for each robot. (a) Robots R_1, R_2 and R_3 . (b) Robots R_4, R_5 and R_6 .

Figure 18 shows the evolution of the potential field for the six fictional robots. A reciprocity can be observed between potential fields. This allows observation of the interaction between robots in the event of possible collisions. Thus it can be seen that in $t = 14$ (s) tot = 17 (s) there is a possible collision between R_1 and R_5 . $t = 29$ (s) tot = 31 (s) there is a collision between R_2 and R_6 . The same occurs in $t = 30$ (s) tot = 33 (s) where there is a collision between R_1 and R_4 , which corresponds to the observed trajectories in Fig 13.



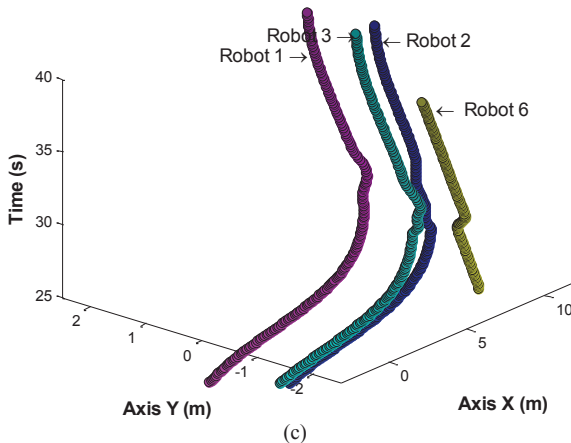


Figure 19. Evolution of time-parameterized trajectories training for the three formation robots with the robots in the environment. (a) The three formation robots R_4 (b) The three formation robots with R_5 (c) The three formation robots with R_6 .

This verifies that the peak of the error control is lower in the second experiment than in first experiment, since R_4 , R_5 and R_6 robots contain obstacle avoidance algorithms and react to the presence of a possible collision with a formation. Figure 19 shows the evolution of the time-parameterized trajectories of the formation robots and robots in the environment. It can be seen that the formation robots avoid a collision with the environment robots. It leads to conclude that there are no collisions between the environment robots and the formation robots, or between the formation robots themselves. The required sensors for the implementation of the real experiments would be a laser sensor mounted on each robot to detect the position of the obstacles, and the positions of the robots are obtained using odometry.

6. CONCLUSIONS

This paper has developed a controller capable of working with multiple-control objectives using the definition of null space. The control objectives are such that the robot formation meets the objectives of shape and posture. (trajectory tracking, position and angle) and the avoidance of static and dynamic obstacles. Potential fields and temporal variations were used to model the dynamics of the obstacles to avoid collisions with the formation. The main contribution of the paper is to present a methodology considering multiple-control objectives using the null space of a Jacobian matrix associated with the definition of an artificial potential and its temporal variation linked to the primary target. The method does not present problems with the existence of local minimums and considers the dynamics of obstacles in motion. Another contribution is the use of the same controller for semi-structured environments with multiple robots having different control tasks. The simulations proved the efficacy of the proposed algorithms. As future work, experimental testing with real robots is expected to contribute to the validation of the proposed controllers.

REFERENCES

- [1] G. Antonelli, F. Arrichiello, and S. Chiaverini. The null-space-based behavioral control for mobile robots. In IEEE International Symposium on Computational Intelligence in Robotics and Automation (CIRA), pages 15–20, 2005.
- [2] G. Antonelli, F. Arrichiello, and S. Chiaverini. The null-space-based behavioral control for autonomous robotic systems. Intelligent Service Robotics, 1(1):27–39, 2008.
- [3] G. Antonelli, F. Arrichiello, and S. Chiaverini. Experiments of formation control with multirobot systems using the null-space-based behavioral control. IEEE Transactions on Control Systems Technology, 17(5):1173–1182, 2009.
- [4] G. Antonelli and S. Chiaverini. Kinematic control of platoons of autonomous vehicles. IEEE Transactions on Robotics, 22(6):1285–1292, 2006.
- [5] T. Balch and R.C. Arkin. Behavior-based formation control for multirobot teams. IEEE Transactions on Robotics and Automation, 14(6):926–939, 1998.
- [6] T.D. Barfoot and C.M. Clark. Motion planning for formation of mobile robots. Robotics and Autonomous Systems, 46(2):65–U78, 2004.
- [7] J. Chen, D. Sun, J. Yang, and H. Chen. Leader” Ufollower formation control of multiple non-holonomic mobile robots incorporating a receding-horizon scheme. The International Journal of Robotics Research, 29(6):727–747, 2010.
- [8] L. Consolini, F. Morbidi, D. Prattichizzo, and M. Tosques. Leader-follower formation control of nonholonomic mobile robots with input constraints. Automatica, 40(5):1343–1349, 2008.
- [9] N. Hogan. Impedance control: An approach to manipulation. ASME Journal of Dynamic Systems, Measurement, and Control, 107:1–23, March 1985.
- [10] O. Khatib. Real time obstacle avoidance for manipulators and mobile robots. The International Journal of Robotics Research, 5(1):90–98, 1986.
- [11] Y. Koren and J. Borenstein. Potential field methods and their inherent limitations for mobile robot navigation. In Proceedings of the IEEE conference on Robotics and Automation, pages 1398–1404, Sacramento, California, April 1991.
- [12] J. Liu and J. Wu. Multiagent Robotic Systems. CRC Press, 2001.
- [13] I. Mas, O. Petrovic, and C. Kitts. Cluster space specification and control of a 3-robot mobile system. In Proceedings of the 2008 IEEE International Conference on Robotics and Automation (ICRA'08), pages 3763–3768, 2008.
- [14] F. Michaud, D. Letourneau, M. Guilbert, and J.M. Valin. Dynamic robot formations using directional visual perception. In IEEE/RSJ International Conference on Intelligent Robots and Systems, volume 3, pages 2740–2745, 2002.
- [15] H. G. Tanner, G. J. Pappas, and V. Kumar. Leader-to-formation stability. IEEE Transactions on Robotics and Automation, 20(3):443 – 455, June 2004.
- [16] V.T.L. Rampinelli, A.S. Brandao, F.N. Martins, M. Sarcinelli-Filho, and R. Carelli. A multi-layer control scheme for multirobot formations with obstacle avoidance. In International Conference on Advanced Robotics (ICAR), pages 1–6, 2009.
- [17] T. Suzuki, T. Sekine, T. Fujii, H. Asama, and I. Endo. Cooperative formation among multiple mobile robot teleoperation in inspection task. In Proceedings of the 39th IEEE Conference on Decision and Control, 2000., volume 1, pages 358 – 363, 2000.
- [18] C.R. Weisbin, J. Blitch, D. Lavery, E. Krotkov, C. Shoemaker, L. Matthies, and G. Rodriguez. Miniature robots for space and military issions. IEEE Robotics & Automation Magazine, pages 9 – 18, September 1999.
- [19] C. Cruz, “Control de Formacion de Robots Móviles”, Tesis doctoral, cap. 2, diciembre 2006.

Appendix A: FIRST APPENDIX

Now the stability of the position errors is analyzed. From (4) for n_{robots} robots $\dot{X}_p = J_r U$ arises, assuming perfect velocity tracking ($U \equiv U_c$) thus:

$$\dot{X}_p = J_f^+ (\dot{q}_{fc} + \dot{q}_{obc}) + (I - J_f^+ J_f) \dot{X}_{pc} \quad (30)$$

replacing (13) in (30):

$$J_p^+ \dot{q}_p = J_f^+ (\dot{q}_{fc} + \dot{q}_{obc}) + (I - J_f^+ J_f) \dot{X}_{pc} \quad (31)$$

Multiplying both members of equality by $J_2 = I - J_f^+ J_f$ and developing

$$J_2 J_p^+ \dot{q}_p = J_2 J_f^+ (\dot{q}_{fc} + \dot{q}_{obc}) + J_2 (I - J_f^+ J_f) \dot{X}_{pc}$$

as $J_2 J_f^+ = 0$

$$\begin{aligned} J_2 J_f^+ &= (I - J_f^+ J_f) J_f^+ \\ &= J_f^+ - J_f^+ J_f J_f^+ \\ &= J_f^+ - J_f^+ J_f J_f^T (J_f J_f^T)^{-1} \\ &= J_f^+ - J_f^+ = 0 \end{aligned}$$

then:

$$J_2 J_p^+ \dot{q}_p = J_2 \dot{X}_{pc}$$

replacing \dot{X}_{pc} (24):

$$J_2 J_p^+ \dot{q}_p = J_2 J_p^+ (\dot{q}_{pd} + K_p \tanh \tilde{q}_p)$$

developing:

$$J_2 J_p^+ (\dot{q}_p + K_p \tanh \tilde{q}_p) = \mathbf{0}$$